Ann Microbiol (2015) 65:1597–1606
DOI 10.1007/s13213-014-0999-4

ORIGINAL ARTICLE

Cloning and characterization of a differentially expressed mitochondrial manganese superoxide dismutase gene from *Pleurotus ostreatus*

Chaomin Yin · Wenxian Zhao · Jihong Zhu · Liesheng Zheng · Liguo Chen · Aimin Ma

Received: 4 March 2014 / Accepted: 3 November 2014 / Published online: 20 November 2014
© Springer-Verlag Berlin Heidelberg and the University of Milan 2014

Abstract Manganese-containing superoxide dismutase (Mn-SOD) is one of the most important superoxide dismutases found in many eukaryotes and bacteria. In this study, the full-length cDNA of mitochondrial manganese superoxide dismutase from *Pleurotus ostreatus* (PoMn-SOD) was obtained. It contained 776 nucleotides with an open reading frame (ORF) of 663 bp, encoding 220 amino acid residues. The deduced amino acid sequence showed high identity with the sequences of other basidiomycetous Mn-SODs from *Trametes versicolor* (71 %) to *Laccaria bicolor* (77 %). Quantitative real-time PCR (RT-PCR) analysis revealed that PoMn-SOD gene transcripts were abundant in the stage of young fruit bodies and mature fruit bodies. The up-regulation of the PoMn-SOD gene suggested that it was developmental regulated and could play an important role in antagonizing environmental stresses. In addition, another isoform of Mn-SOD was detected by a non-denaturing polyacrylamide gel electrophoresis (PAGE) approach and the highest total Mn-SOD activity (203.9 U/mg) was observed in the stage of mature fruit bodies. These data could provide important reference for functional study of the PoMn-SOD gene and may benefit biotechnological production of Mn-SOD in the future.

C. Yin · W. Zhao · J. Zhu · A. Ma (✉)
College of Food Science and Technology,
Huazhong Agricultural University, Wuhan 430070, China
e-mail: aiminma@mail.hzau.edu.cn

L. Zheng · L. Chen
College of Plant Science and Technology,
Huazhong Agricultural University, Wuhan 430070, China

A. Ma
Key Laboratory of Agro-Microbial Resources and Utilization,
Ministry of Agriculture, Wuhan 430070, China

Keywords *Pleurotus ostreatus* · Manganese-containing superoxide dismutase · Bioinformatics analysis · Homology modeling · Quantitative real-time PCR · Non-denaturing polyacrylamide gel electrophoresis

Introduction

Pleurotus ostreatus (Jacq.:Fr.) kummer is the second largest commercially cultivated edible mushroom in the world. Under appropriate conditions, the mycelia of *P. ostreatus* in cultivating substrates will develop into primordia and subsequently into mature fruit bodies (Sánchez 2010). During these developmental stages, cells of *P. ostreatus* require a large amount of ATP, which results in the intense reduction of oxygen.

Oxidative stress is the adverse effect of oxidants on physiological function and occurs when abnormally high levels of reactive oxygen species (ROS) are generated during oxygen metabolism (Liu et al. 2012). Aberrant production of ROS, including superoxide anion (O_2^-), hydroxyl radical (·OH), and hydrogen peroxide (H_2O_2) normally generated by normal cell metabolism and chemical or environmental stresses, can cause oxidative damage to many cellular components such as lipids, protein, and DNA, which will lead to cell death (Dong et al. 2009; Holley et al. 2011). Superoxide dismutase (SOD) is the primary ROS detoxifying enzyme in cells that catalyzes the dismutation of superoxide radicals to hydrogen peroxide and molecular oxygen. According to the metal embedded at the active site of this enzyme, it can be divided into copper- and zinc-containing superoxide dismutase (Cu/Zn-SOD), iron-containing superoxide dismutase (Fe-SOD), and manganese-containing superoxide dismutase (Mn-SOD) (Wang et al. 2010). Cu/Zn-SODs are mostly found in eukaryotes and rarely in bacteria (Wang et al. 2010). Fe-SODs are present in prokaryotes and within chloroplasts of some plants

(Hadji Sfaxi et al. 2012). Mn-SODs exist in the mitochondria and/or cytoplasm of many species, typically as tetramers and dimers, respectively (Iranzo 2011). Mitochondria Mn-SODs are firstly synthesized as a precursor protein in cytoplasm and then imported into the mitochondrial matrix after cleavage of its signal peptide (Ekanayake et al. 2006). The mitochondrial matrix is the major site producing cellular energy and the main source for single-electron reduction of O_2 to produce O_2^-. Therefore, Mn-SODs are thought to be a major scavenger of ROS in the mitochondrial matrix (Lin et al. 2009). This is vital for healthy aerobic life, and lack of this enzyme is lethal (Miriyala et al. 2011; Holley et al. 2012).

Since Ravindranath and Fridovich (1975) first isolated Mn-SOD from *Saccharomyces cerevisiae*, more and more fungal Mn-SODs have been documented. For instance, elimination of the Mn-SOD gene from the genome of *Saccharomyces cerevisiae* resulted in rapid death in the stationary phase and increased susceptibility to oxidative stress (Longo et al. 1999; O'Brien et al. 2004). Knock-out Mn-SOD *Candida albicans* and *Schizosaccharomyces pombe* increased the sensitivity to various stresses compared to wild-type strains (Jeong et al. 2001; Hwang et al. 2003). Mn-SOD over-expression in *Beauveria bassiana* significantly increased the virulence to *Spodoptera litura* larvae and enhanced tolerance to the stress of chemical oxidation and UV-B irradiation (Xie et al. 2010). Additionally, over-expression of Mn-SOD in yeast led to a longer chronological life span (Harris et al. 2003). Up to now, we know little about Mn-SOD from the oyster mushroom.

In our previous work, a 310 bp 3′ cDNA fragment of mitochondrial manganese superoxide dismutase gene from *P. ostreatus* (PoMn-SOD) was obtained with a differential screening method (Yin et al. 2012). In this study, we report the full-length cloning, characterization and expression analysis of the PoMn-SOD gene. We also investigate the total Mn-SOD activity of cell-free extracts in *P. ostreatus*.

Materials and methods

Strains and culture conditions

Pleurotus ostreatus Pd739 was provided by Laboratory of Food Microbiology, Huazhong Agricultural University, and maintained on potato dextrose agar (PDA, Difco, USA) slant at room temperature. Mycelium and fruit bodies were produced as previously described (Joh et al. 2007). Samples from four different developmental stages including vegetative mycelia, primordia (2–3 mm in diameter), young fruiting bodies (no gill formed), and mature fruiting bodies (gills formed and spores dispersed) were harvested and stored at −70 °C (Ma et al. 2007). *Escherichia coli* DH5α (Takara, Dalian, China) was cultured in Luria-Bertani medium (LB, Difco, USA) at 37 °C for standard bacterial cloning.

Full-length cDNA and genomic DNA cloning

Total RNA was extracted with RNAiso™ Plus (Takara, Dalian, China), and then reverse transcribed into the first-strand cDNA using SMART™ RACE cDNA Amplification Kit (Clontech, American). The 5′ cDNA of PoMn-SOD was amplified using the specific primer MS-R5 (Table 1) combined with the universal primer (UPM in Table 1) in a 50 μl reaction system. The thermal cycling conditions were as follows: 94 °C for 10 min followed by 35 cycles at 94 °C for 30 s, 58 °C for 30 s, and 72 °C for 1 min, with a final extension at 72 °C for 10 min (Yin et al. 2014). The PCR product was purified with AxyPrep™ DNA Gel Extraction Kit (Axygene, Hangzhou, China), then cloned into pMD®18-T (Takara, Dalian, China) and transformed into *Escherichia coli* DH5α by heat shock. cDNA inserts isolated from positive clones were sequenced (Invitrogen, Shanghai, China). The full-length cDNA was cloned into *E. coli* DH5α using a pair of gene-specific primers, MS-FS and MS-FA (Table 1), designed from the full-length PoMn-SOD cDNA sequence obtained by joining the fragments of 5′ and 3′ ends with DNAMAN 6.0.

Genomic DNA was extracted with CTAB method (Ma et al. 2007), and used to amplify the PoMn-SOD genomic sequence using gene-specific primers MS-FS and MS-FA (Table 1). Fifty-microliter reaction mixtures were used in the PCR reaction and the conditions were as follows: 94 °C for 10 min followed by 35 cycles at 94 °C for 30 s, 56 °C for 30 s, and 72 °C for 1 min, with a final extension at 72 °C for 10 min (Yin et al. 2014). The PCR products were cloned into pMD®18-T and transformed into *E. coli* DH5α for sequencing.

Bioinformatics analysis

Sequence similarity analysis was conducted using BLAST from NCBI (http://www.ncbi.nlm.nih.gov/BLAST/). Open reading frame (ORF) was found using NEW GENSCAN (http://genes.mit.edu/GENSCAN.html). Mitochondrion transit peptide and subcellular localization were predicted using TargetP V1.1 (www.cbs.dtu.dk/services/TargetP/) and PSORT Prediction (http://psort.hgc.jp/form.html). Asparagine-linked glycosylation sites were determined by NetNGlyc 1.0 (http://www.cbs.dtu.dk/services/NetNGlyc). Protein motifs were identified using MOTIF Search (http://www.genome.jp/tools/motif/) and the Conserved Domain Database from NCBI (http://www.ncbi.nlm.nih.gov/Structure/cdd/wrpsb.cgi). Theoretical isoelectric point and molecular weight were predicted using Compute PI/MW (http://expasy.org/tools/protparam.html). Multi-sequence alignment was generated using CLUSTALX and phylogenetic analysis was performed using MEGA 5.0. Homology modeling was performed using the Discovery studio 2.5. Protein secondary structure was predicted using the SOPMA

secondary structure prediction method (http://npsa-pbil.ibcp.fr/cgi-bin/npsa_automat.pl?page=npsa_sopma.html). The protein hydropathy profile was determined by ProtScale (http://web.expasy.org/protscale/).

Quantitative RT-PCR expression analysis

The first strand cDNA was synthesized from total RNA of vegetative mycelia, primordia, young fruit bodies, and mature fruit bodies using PrimeScript RT Reagent Kit with gDNA Eraser (Takara, Dalian, China). For ascertaining the expression levels of the PoMn-SOD gene in different stages, quantitative real-time PCR was performed on the ABI ViiA7 Real-Time PCR System (Applied Biosystems, Foster City, CA, USA) using α-tubulin gene as endogenous control. Specific primers for α-tubulin gene (Table 1) and Mn-SOD gene (Table 1) has been synthesized (Invitrogen, Shanghai, China). RT-PCR was performed using SYBR *Premix Ex Taq*™ (Takara, Dalian, China) according to the manufacturer's instructions. Twenty-microliter reaction mixtures were used in the RT-PCR reaction and conditions were as follows: 95 °C for 30 s followed by 40 cycles at 95 °C for 5 s and 60 °C for 31 s. Each RT-PCR reaction was carried out with three replicates, and the data from the samples were analyzed with the Relative Manager Software (Applied Biosystems, Foster City, CA, USA) to estimate transcript levels of each sample using the $2^{-\Delta\Delta Ct}$ method.

Preparation of cell-free extracts

Cell-free extracts of vegetative mycelia, primordia, young fruit bodies, and mature fruit bodies were prepared by mortar and pestle in the presence of liquid N_2. About 0.3-g cell lysates were resuspended in 1 ml of Native Solution (50 mM phosphate buffer, pH 7.8, 0.1 mM EDTA). The homogenate was sonicated (400 W, 20 s×3) in an ice bath, and then centrifuged at 12,000×*g* for 20 min at 4 °C. The supernatants were collected as crude enzyme and used for biochemical assays. Protein concentration was determined by the Bradford method with BSA as a standard (Bradford 1976).

Non-denaturing polyacrylamide gel electrophoresis

Electrophoresis was carried out with 1.5 mm of 12 % polyacrylamide mini-slab gel in standard tris-glycine buffer (pH 8.3) at room temperature according to a modified procedure (Gabriel 1971). Twenty-microliter samples were loaded into each well and then electrophoresed at 60 V through the 5 % stacking gel for 45 min and 120 V through the separating gel for 120 min. After electrophoresis, a modified photochemical method was used to locate SOD activities on gels (Beauchamp and Fridovich 1971; Elstner and Heupel 1976). The gel was first soaked in 25 ml of 2.45 mM NBT for 45 min, briefly washed, then soaked in the dark in 30 ml of 50 mM potassium phosphate buffer (pH 7.8) containing 28 mM TEMED and 0.028 mM riboflavin for another 30 min. The gel was illuminated on a light box with an intensity of 30 μmol photons m^{-2} s^{-1} until activity bands were seen as pale zones on the dark blue background. The gels were scanned or photographed, and then kept in 50 mM phosphate buffer in complete darkness.

Mn-SOD assay of cell-free extracts

To determine the Mn-SOD activity of cell-free extracts, Cu/Zn-SOD and Mn-SOD Assay Kit with WST-1 (Beyotime Institute of Biotechnology, Jiangsu, China) was applied. Measurements were performed with a Thermo Multiskan Mk3 (Thermo Fisher Scientific, USA) at 450 nm in 96-well microtitre plates. In 1 unit of SOD, the 50 % inhibition activity of SOD was determined by diluting the sample to different concentrations.

Results

Sequence analysis of PoMn-SOD gene

In our previous work, a 310 bp 3′ cDNA fragment of the PoMn-SOD gene was isolated (Yin et al. 2012). By 5′ RACE

Table 1 Primers for PCR amplification in this study

Primer name	Sequence (5′→3′)	Description
MS-R5	AAGGGGTCCTGGTTGGGGGTCGTGGT	Specific primer of PoMn-SOD gene for 5′ RACE PCR
UPM (long)	CTAATACGACTCACTATAGGGCAAGCAGTGGTATC AACGCAGAGT	Universal primer for 5′ RACE PCR
UPM (short)	CTAATACGACTCACTATAGGGC	
MS-FS	ACTCATTCCCGTTCTACCAT	Primers of PoMn-SOD gene for cDNA and genomic DNA amplification
MS-FA	CGCTGCTAAGTTCATCACAAG	
RAPF	GGTTTGAACGCTGCTGAG	Primers of PoMn-SOD gene for quantitative real-time PCR
RAPR	AGTTTGCCTCCGTCACCG	
α-tubulinF	CCGCTATCTCACCGTCGC	Primers of α-tubulin gene for quantitative real-time PCR
α-tubulinR	GTTCTTGGATGGCGGTCG	

PCR reaction, we obtained a 516 bp fragment with a gene-specific primer MS-R5 after trimming the adaptors using DNAMAN 6.0. Finally, we obtained a full-length PoMn-SOD cDNA (GenBank Accession No. KF768153) consisting of 776 nucleotides with an open reading frame (ORF) of 663 bp, a 5′ -UTR region of 30 bp, and a 3′ -UTR region of 83 bp containing the poly A tail. The ORF encodes a protein of 220 amino acid residues including a mitochondrion transit peptide (aa1-25) and two putative *N*-glycosylation sites located at the amino acid residues 95–98 (−N-H-S-L-) and 137–140 (−N-T-T-T-). The theoretical isoelectric point (pI) and molecular weight (M_w) of the putative mature polypeptide are 6.8 and 21.8 kDa, respectively. The deduced amino acid sequence displays the characteristic primary structure of typical superoxide dismutase.

Multiple sequence alignment and phylogenetic analysis

Similarity analysis using the NCBI BLAST program showed that the deduced amino acid sequence of PoMn-SOD possessed homology with manganese superoxide dismutases from *Laccaria bicolor* (77 %, XP_001878774), *Coniophora puteana* (75 %, EIW74749), *Stereum hirsutum* (75 %, EIM79240), *Coprinopsis cinerea* (74 %, XP_001837757), *Fomitiporia mediterranea* (73 %, EJD04865), *Auricularia delicata* (73 %, EJD39831), *Trametes versicolor* (71 %, EIW64309) (Fig. 1). To examine the phylogenetic relationship of PoMn-SOD with other homologous manganese superoxide dismutases, a phylogenetic tree was constructed based on the amino acid sequences from 17 species. Protein distance-based phylogenetic analysis showed the PoMn-SOD branched between *S. hirsutum* and *A. delicata* (Fig. 2).

The structure of the PoMn-SOD gene

The PoMn-SOD gene (GenBank Accession No. KF768154) consists of 1,031 bp without the untranslated region (UTR). It contains seven exons and six introns (113–162, 50 bp; 327–377, 51 bp; 556–607, 52 bp; 671–721, 51 bp; 773–885, 113 bp; 909–959, 51 bp). The first intron (TA-GG) and the

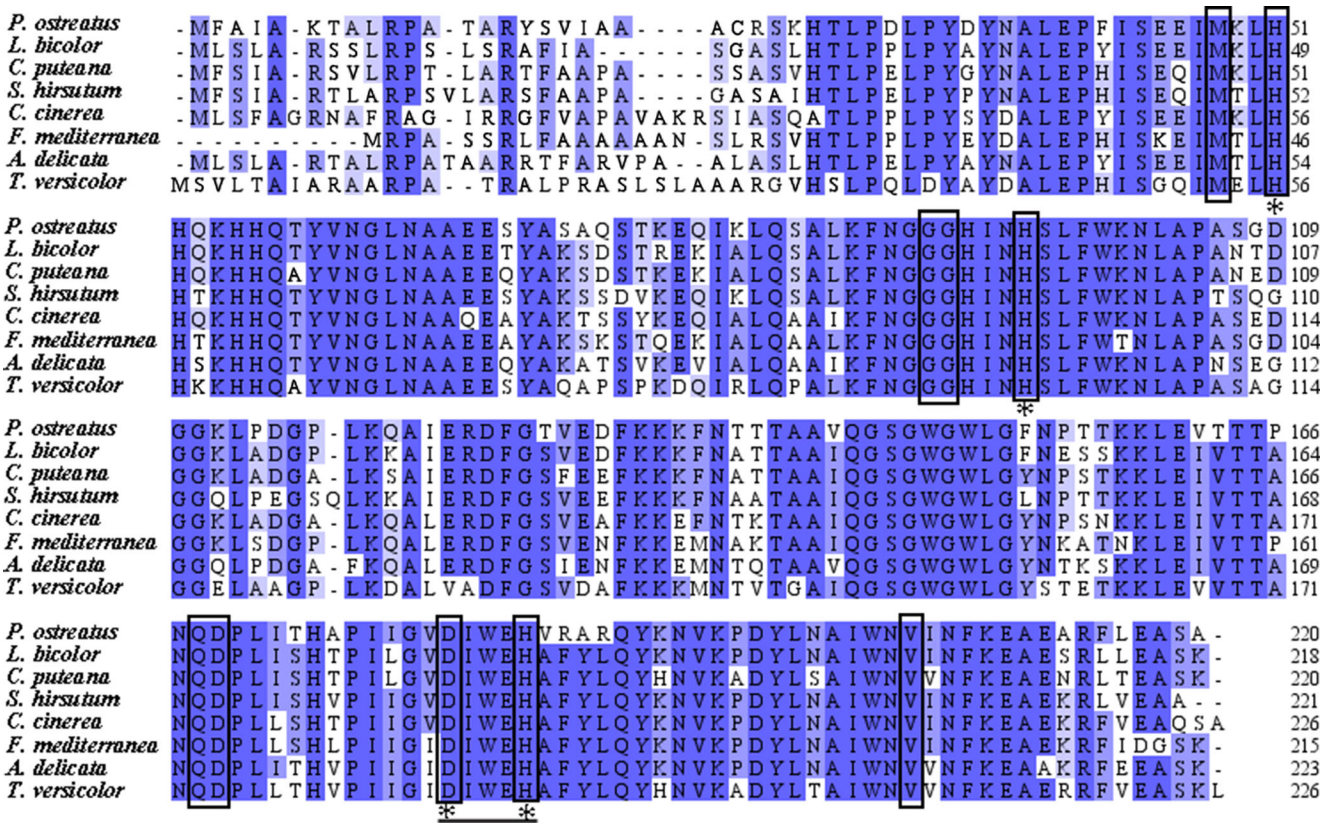

Fig. 1 Multiple amino acid sequence alignment of the PoMn-SOD with homologues from other basidiomycetes. Accession numbers of amino acid sequences were as follows: *L. bicolor* Mn-SOD (XP_001878774), *Coniophora puteana* Mn-SOD (EIW74749), *Stereum hirsutum* Mn-SOD and Fe-SOD (EIM79240), *Coprinopsis cinerea* Mn-SOD (XP_001837757), *F. mediterranea* Mn-SOD (EJD04865), *A. delicata* Mn-SOD (EJD39831), *T. versicolor* mitochondrial SOD (EIW64309). Conservative residues are shown in dark blue boxes, identical residues in light blue boxes, and unrelated residues have a white background. The amino acids characteristics of the Mn-SODs are boxed (Parker and Blake 1988; Graeff-Wohlleben et al. 1997). The Mn-SOD signature of the decapod crustaceans (DIWEH) is underlined. Four residues involved in the metal center are boxed with*. Amino acid numbers are shown on the right

sixth intron (GT-AG) splice motifs are common in organisms. Some special intron splice motifs, such as the second intron (AA-GT), the third intron (TT-GG), the fourth intron (GC-AG), and the fifth intron (TT-AC), have also been found.

Secondary structure, hydropathy profile and homology modeling of PoMn-SOD

We predicted the PoMn-SOD secondary structure using the SOPMA software and the results showed the PoMn-SOD was a highly alpha-helix protein. In addition to those in the N- and C-terminals, there were two big alpha helices in the center of the protein (Fig. 3a). We analyzed the PoMn-SOD hydropathy profile using the ProtScale, the results showed that most of the peaks were below zero (score <0), which meant the regions of these peaks represented highly hydrophilic areas (Fig. 3b). The three-dimensional structure modeling of the PoMn-SOD was conducted using the software Discovery studio 2.5. According to the homology search in Worldwide Protein Data Bank (WWPDB), the structure of *Caenorhabditis elegans* mitochondrial Mn-SOD (PDB ID: 3 DC6) was identified as the best template for homology modeling. The protein model consists of 11 helices and three beta-strands, which shows the PoMn-SOD is a protein with highly helices. This is consistent with the results of secondary structure prediction (Fig. 4).

Differential expression analysis of the PoMn-SOD gene

In order to determine the expression levels of PoMn-SOD gene transcripts in different developmental stages, quantitative RT-PCR was performed using the first-strand cDNA from vegetative mycelia, primordia, young fruit bodies, and mature fruit bodies of *P. ostreatus*. The expression level in primordia was used as a reference, and the highest level of PoMn-SOD gene expression was observed in the stage of mature fruit bodies (12.9-fold), followed by young fruit bodies (4.1-fold) and vegetative mycelia (1.5-fold) (Fig. 5a).

SOD activity of cell-free extracts

The SOD activity of cell-free extracts from different developmental stages of *Pleurotus ostreatus* was resolved into multi-bands through non-denaturing PAGE (Fig. 5b). They were tested for their susceptibility to 2 mM H_2O_2. We found that band I and band II (Fig. 5c) were insensitive to H_2O_2, indicating that they were Mn-SODs (Cheng et al. 2012). This suggested that another Mn-SOD isoenzyme was also expressed during

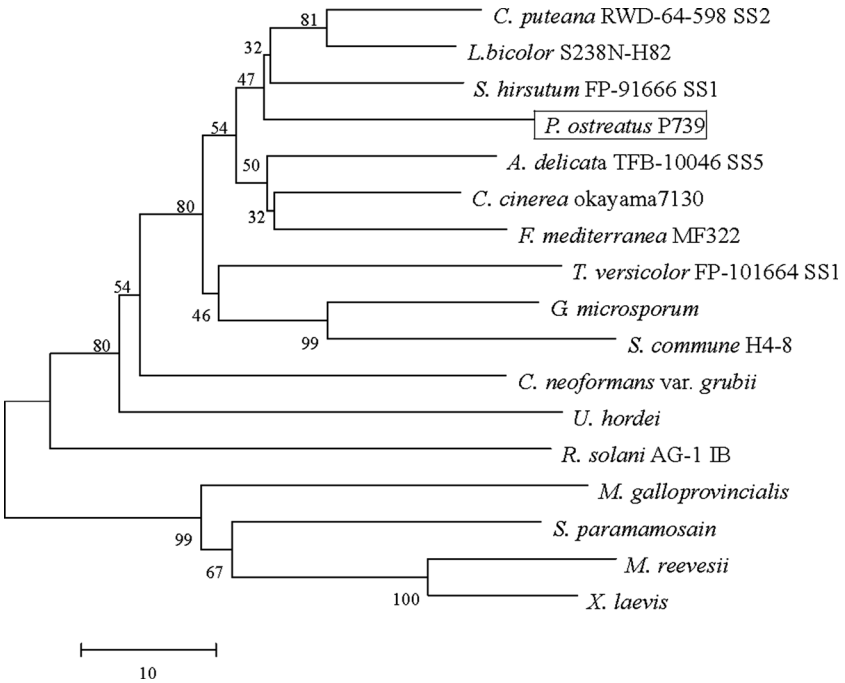

Fig. 2 A molecular phylogenetic tree of Mn-SOD generated by the neighbor-joining (NJ) method using MEGA 6.1. An unrooted phylogenetic tree was generated based on the alignment of the amino acid sequences from 17 species. One thousand bootstrap replicates were calculated, and bootstrap values are shown at each node. Nodes were collapsed to a single horizontal line whenever statistical support was less than 60 %. The scale bar indicates an evolutionary distance of amino acid substitutions per position. Accession numbers of amino acid sequences were as follows: *Coniophora puteana* (EIW74749) *L. bicolor* (XP_001878774), *Stereum hirsutum* (EIM79240), *A. delicate* (EJD39831), *Coprinopsis cinerea* (XP_001837757), *F. mediterranea* (EJD04865), *T. versicolor* (EIW64309), *Ganoderma microsporum* (Q92429), *Schizophyllum commune* (XP_003036155), *Cryptococcus neoformans* (AAW56834), *Ustilago hordei* (CCF48021), *Rhizoctonia solani* (CCO35898), *Mytilus galloprovincialis* (AFQ32466.1), *Scylla paramamosain* (ACM61856), *Mauremys reevesii* (AFX95919), *Xenopus laevis* (NP_001083968)

different developmental stages. However, we could not rule out the possibility that isoenzyme II (band II) was the proteolytic product of isoenzyme I (band I). Among the bands, isoenzyme I (band I) covered around 50 % of the total SOD activity in the cell-free extracts (Fig. 5b and c).

Cell-free extract based Mn-SOD assay

The Cu/Zn-SOD and Mn-SOD Assay Kit were used to determine the Mn-SOD activity in the different developmental stages of *Pleurotus ostreatus*. Fig. 5d showed the highest level

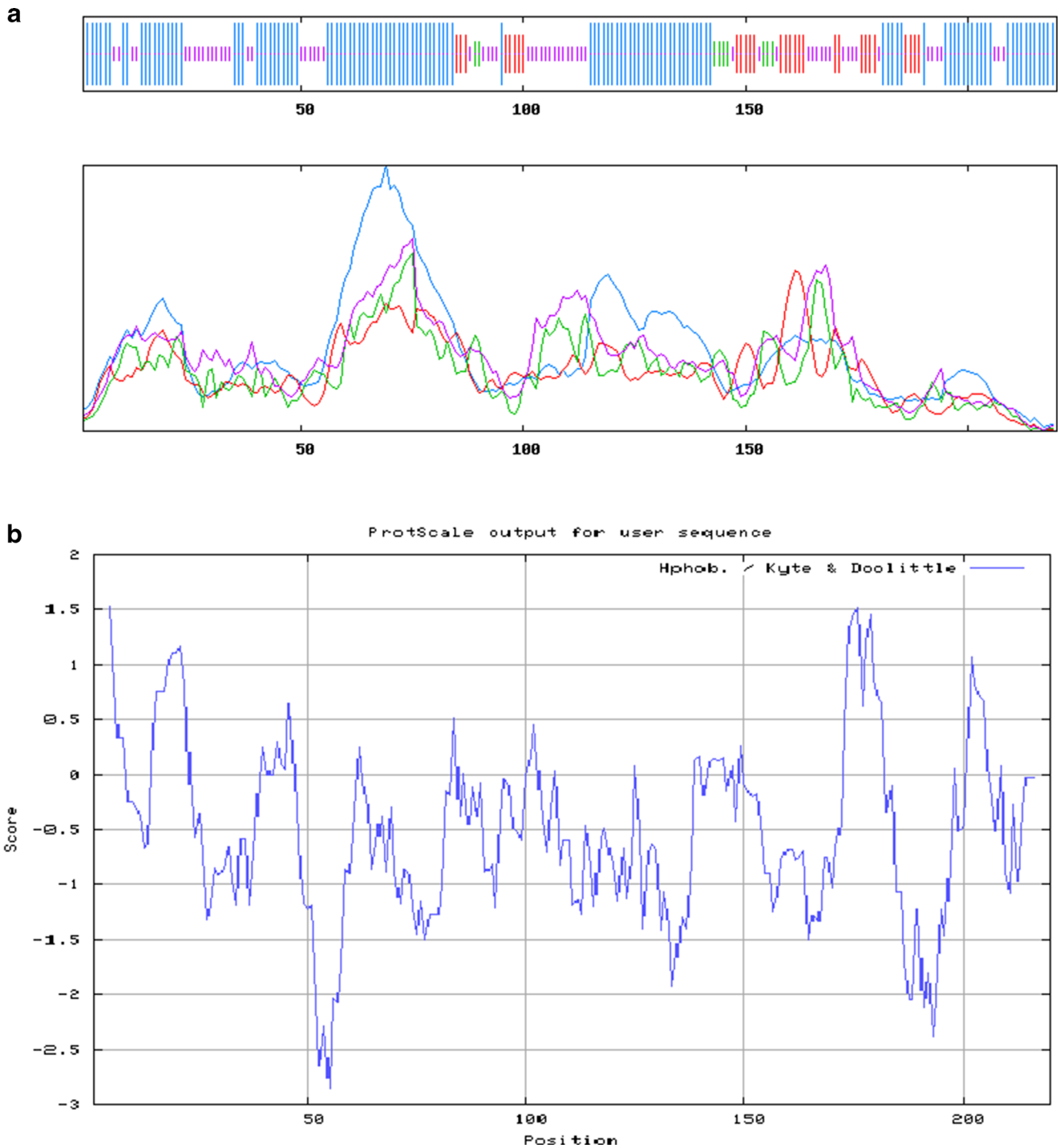

Fig. 3 The secondary structure and the hydropathy profile of PoMn-SOD. **a** is the result of the secondary structure prediction (the blue line represents the alpha helix, the red line represents the extended strand, the green line represents the beta turn, and the orange line represents the random coil). **b** is the hydropathy profile which was calculated according to the Kyte and Doolittle algorithm using a window size of nine amino acid residues

of Mn-SOD activity reaching 203.9 U/mg in the stage of mature fruit bodies, followed by young fruit bodies (152.2 U/mg) and dikaryotic mycelia (122.7 U/mg). The lowest level of Mn-SOD activity was observed in the stage of primordia with the activity of 110.6 U/mg.

Discussion

In this study, we cloned the PoMn-SOD gene and analyzed its expression and enzyme activity during the different development stages of *Pleurotus ostreatus*. The estimated molecular weight (M_w) of mature polypeptide was 21.8 kDa. The molecular weight of PoMn-SOD was similar to that of Mn-SODs from *Chaetomium thermophilum* (Guo et al. 2008), *Thermoascus aurantiacus* var. *levisporus* (Song et al. 2009), and *Bacillus* sp. MHS47 (Areekit et al. 2011). The theoretical isoelectric point (pI) of PoMn-SOD was calculated to be 6.8, which was similar to that of Mn-SODs from *Laternula elliptica* (6.75) (Park et al. 2009), *Thermus thermophilus* HB27 (6.4) (Liu et al. 2011), and *Bambusa oldhamii* (6.78) (Wu et al. 2011).

The extended the N-terminal sequence of PoMn-SOD contains 25 amino acid potential mitochondrial target sequences with a probability of export to mitochondria 0.845 (indicate the strongest prediction) using the TargetP 1.1. This suggests that the PoMn-SOD we cloned is mitochondrial Mn-SOD, not cytosolic Mn-SOD. Twenty-five amino acid signal peptides of Mn-SOD have also been reported in basidiomycetes *Coniophora puteana* (EIW74749) and *Stereum hirsutum* (EIM79240). The function of this presumed signal peptide was reported as the translocation of Mn-SOD into mitochondria (Ekanayake et al. 2006). Mitochondrial Mn-SOD catalyzes the dismutation of superoxide radicals in mitochondria and prevents the disruption of mitochondrial membrane and the damage of proteins and nucleic acids (Kowluru et al. 2006). Thus, it can be deduced that mitochondrial Mn-SOD might play a more important role than cytosolic Mn-SOD in protecting cells from oxidative stresses (Zhang et al. 2007).

Using the protein BLAST program, we found that PoMn-SOD shared significant identity (above 71 %) with Mn-SOD from other homobasidiomycetes (Fig. 1). Most of the regions required for activity are conserved in all compared Mn-SODs including four residues required for coordination of Mn ion (H51, H96, D181, and H185) and the Mn-SOD signature (DIWEH). Fe- and Mn-SODs were assumed to have a common evolutionary origin due to the similarity in their amino acid sequences and three-dimensional protein structures (Parker and Blake 1988). They were unequally distributed throughout the living organisms and located in different cellular compartments (Grace 1990). The Parker and Blake signature sequences specific for Mn-SODs were found in PoMn-SOD, including Gly91, Gly92, Phe99, Gln168, and Asp169 (Parker and Blake 1988). The N- and C-terminal domains typical for the superfamily and a sod A domain were also present in PoMn-SOD.

Protein distance-based phylogenetic analysis of the eukaryotic Mn-SOD amino acid sequences resulted in an unrooted tree in which PoMn-SOD branched between *Stereum hirsutum* and *Auricularia delicata*. As Fig. 2 showed, the Mn-SODs from 17 species could be divided into two clusters. The species in the first cluster belonged to basidiomycota as well as the second one to metazoa. Interestingly, the PoMn-SOD shared above 52 % identity to those Mn-SODs from metazoa. Therefore, we considered that Mn-SODs were evolutionarily conserved for their importance in ROS regulation for healthy aerobic life (Fréalle et al. 2005). Meanwhile, Fukuhara et al. (2002) suggested that Mn-SOD could be a suitable candidate to use as a molecular marker for evolutionary studies since Mn-SOD was present as a single copy in mammals.

In view of the DNA and cDNA sequence alignment of the PoMn-SOD gene, six putative introns were found. The size of introns varied from 50 to 113 bp, and the largest intron was located at the 3′ region. Additionally, the first intron (TA-GG) and the sixth intron (GT-AG) splice motifs are both typical introns based on the consensus splice site and internal sequence for lariat formation (Gurr et al. 1987). In addition, the polyadenylation signal (AATAAA) had not been found in the PoMn-SOD gene, which is similar to the result of Schuren's research (Schuren 1992). We considered that no polyadenylation signal in the PoMn-SOD gene may be caused by the analogous T- or TG-rich motif or other unknown mechanisms.

The predicted secondary structure of PoMn-SOD contained two big alpha helices in the center of the protein

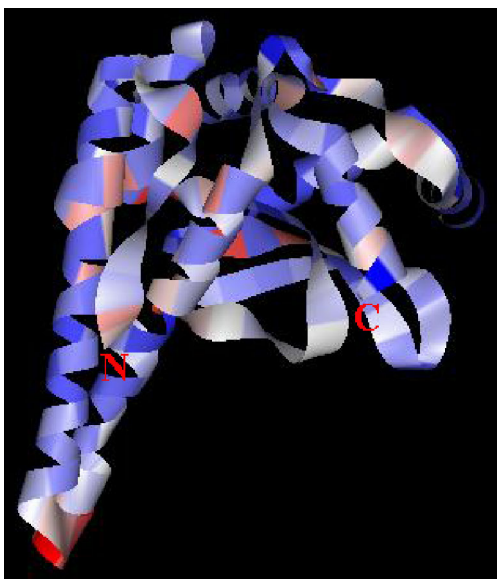

Fig. 4 Homology modeling structure of PoMn-SOD. The N- and C-terminals have been shown

and the corresponding area in the hydropathy profile was highly hydrophilic. The four residues required for coordination of the Mn ion were located in the highly hydrophilic region. Research showed that the active site manganese ion is complexed by the side chains of histidine and aspartic acid residues, forming a trigonal pyramidal coordination polyhedron which will easily interact with substrate by the hydrophilic interaction (Lee et al. 2010). Based on the homology modeling, we found the N-terminus of PoMn-SOD was mainly composed of alpha-helices and the C-terminus consisted of antiparallel beta-sheets and helices. It has been suggested that the observed α1 helical conformation is required to juxtapose the three residues (H51, H55, and Y59), and this arrangement is crucial for Mn-SOD catalysis (Lin et al. 2009).

During different developmental stages of *Pleurotus ostreatus*, we observed that the highest expression levels of the PoMn-SOD gene appeared in the stage of mature fruit bodies, followed by young fruit bodies and vegetative mycelia. Fang et al. (2002) found that the Mn-SOD of plant pathogenic fungus *Colletotrichum graminicola* has the highest expression level in mycelium, which actively produces oval conidia. Blackman et al. (2005) discovered that the *Phytophthora nicotianae* Mn-SOD1 gene is predominantly expressed in vegetative mycelium, but not in zoospores. Cheng et al. (2012) confirmed that edible mushrooms, especially caps, are rich in Mn-SOD when compared to other organisms. The results of these studies are consistent with our findings in *Pleurotus ostreatus*, and we suspected PoMn-SOD might be associated with basidiospore formation. Additionally, changes of Mn-SOD expression during development in several species has been reported, which suggests that development may involve altered levels of ROS production, either as a result of metabolic changes or as a reflection to the role of ROS in signaling (Blackman et al. 2005). The *Pleurotus ostreatus* life-cycle, initiated by spore germination, mycelium growth, primordium formation, and fruit body maturation, depends upon numerous biological events. During these developmental stages, *Pleurotus ostreatus* needs to face

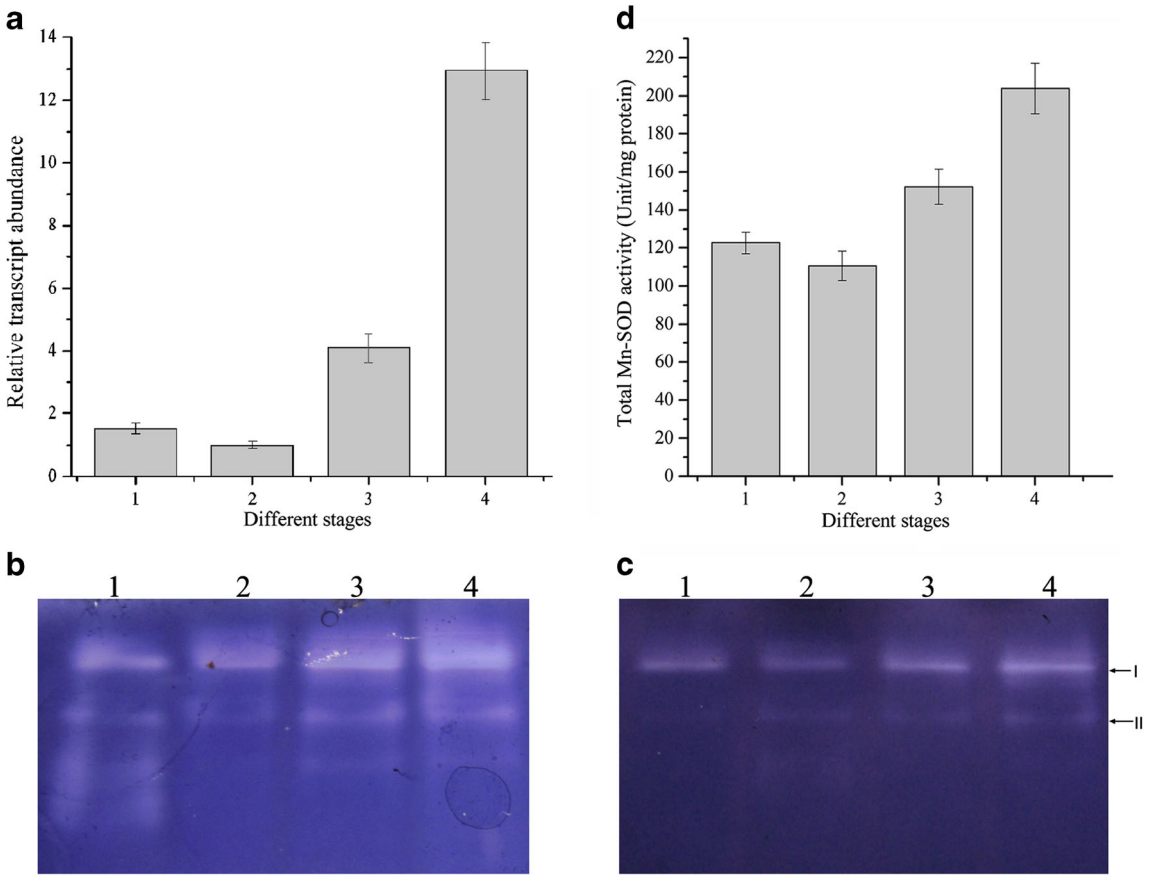

Fig. 5 The relative transcript abundance of PoMn-SOD gene and Mn-SOD activity of *Pleurotus ostreatus* cell-free extracts. **a** is the PoMn-SOD gene expression levels. The expression ratios were calculated according to the $2^{-\Delta\Delta Ct}$ method and the expression level in primordia stage was used as a reference. Bars represent the SDs of three independent replicates. In both assays, the α-tubulin gene was used as an endogenous control. **b** is the SOD isoenzymes revealed by non-denaturing PAGE gel image. **c** is the Mn-SOD isoenzymes revealed by non-denaturing PAGE gel image (two Mn-SOD isoenzymes are indicated by I and II). **d** is the total Mn-SOD activity. Values represent the mean and standard deviation of triplicates. 1–4 represent four developmental stages including vegetative mycelia, primordia, young fruit bodies, and mature fruit bodies, respectively

different environmental stresses, such as UV irradiation, high temperatures, drought, or chemicals that might regulate Mn-SOD gene expression (Gessler et al. 2007).

We conducted non-denaturing PAGE to detect the Mn-SODs. The common SODs could be distinguished for their susceptibility to KCN and H_2O_2. According to Cheng et al. (2012), Cu/Zn-SOD is sensitive to both KCN and H_2O_2, while Fe-SOD is only sensitive to H_2O_2 and Mn-SOD is not sensitive to either of the two chemicals. In our study, at least two Mn-SODs were detected. The gel analysis suggested that the Mn-SOD had different expression levels in different developmental stages. Many fungi expressed Mn-SOD in the cytosolic compartment and mitochondria (Fréalle et al. 2005), so we considered that one of the discovered Mn-SODs might come from the cytosol. We used a Cu/Zn-SOD and Mn-SOD Assay Kit to determine the enzymatic activity of Mn-SOD in *Pleurotus ostreatus*. The total enzymatic activity of Mn-SOD in the different developmental stages was somewhat different, which might be caused by the different expression levels of two Mn-SODs in different developmental stages.

Acknowledgments This work was supported by grants from the National Natural Science Foundation of China (No. 31172011 and No. 30771502). We thank Weifeng Chen for her assistance during the homology modeling.

References

Areekit S, Kanjanavas P, Khawsak P, Pakpitchareon A, Potivejkul K, Chansiri G, Chansiri K (2011) Cloning, expression, and characterization of thermotolerant manganese superoxide dismutase from *Bacillus* sp. MHS47. Int J Mol Sci 12:844–856

Beauchamp C, Fridovich I (1971) Superoxide dismutase: improved assays and an assay applicable to acrylamide gels. Anal Biochem 44: 276–287

Blackman LM, Mitchell HJ, Hardham AR (2005) Characterisation of manganese superoxide dismutase from *Phytophthora nicotianae*. Mycol Res 109:1171–1183

Bradford MM (1976) A rapid and sensitive method for the quantitation of microgram quantities of protein utilizing the principle of protein-dye binding. Anal Biochem 72:248–254

Cheng GY, Liu J, Tao MX, Lu CM, Wu GR (2012) Activity, thermostability and isozymes of superoxide dismutase in 17 edible mushrooms. J Food Compos Anal 26:136–143

Dong C, Li G, Li Z, Zhu H, Zhou M, Hu Z (2009) Molecular cloning and expression analysis of an Mn-SOD gene from *Nelumbo nucifera*. Appl Biochem Biotechnol 158:605–614

Ekanayake PM, Kang HS, De Zyosa M, Jee Y, Lee YH, Lee J (2006) Molecular cloning and characterization of Mn-superoxide dismutase from disk abalone (*Haliotis discus discus*). Comp Biochem Physiol B Biochem Mol Biol 145:318–324

Elstner EF, Heupel A (1976) Inhibition of nitrite formation from hydroxylammonium chloride: a simple assay for superoxide dismutase. Anal Biochem 70:616–620

Fang GC, Hanau RM, Vaillancourt LJ (2002) The SOD2 gene, encoding a manganese-type superoxide dismutase, is up-regulated during conidiogenesis in the plant-pathogenic fungus *Colletotrichum graminicola*. Fungal Genet Biol 36:155–165

Fréalle E, Noël C, Viscogliosi E, Camus D, Dei-Cas E, Delhaes L (2005) Manganese superoxide dismutase in pathogenic fungi: an issue with pathophysiological and phylogenetic involvements. FEMS Immunol Med Microbiol 45:411–422

Fukuhara R, Tezuka T, Kageyama T (2002) Structure, molecular evolution, and gene expression of primate superoxide dismutases. Gene 296:99–109

Gabriel O (1971) Locating enzymes on gels. In: Colowick SP, Kaplan NO (eds) Methods in Enzymology (vol 22). Academic, New York, p 578

Gessler NN, Averyanov AA, Belozerskaya TA (2007) Reactive oxygen species in regulation of fungal development. Biochemistry (Mosc) 72:1091–1109

Grace SC (1990) Phylogenetic distribution of superoxide dismutase supports an endosymbiotic origin for chloroplasts and mitochondria. Life Sci 47:1875–1886

Graeff-Wohlleben H, Killat S, Banemann A, Guiso N, Gross R (1997) Cloning and characterization of an Mn-containing superoxide dismutase (SodA) of *Bordetella pertussis*. J Bacteriol 179:2194–2201

Guo FX, Shi-Jin E, Liu SA, Chen J, Li DC (2008) Purification and characterization of a thermostable MnSOD from the thermophilic fungus *Chaetomium thermophilum*. Mycologia 100:375–380

Gurr SJ, Unkles SE, Kinghorn JR (1987) The structure and organization of nuclear genes in filamentous fungi. In: Kinghorn JR (ed) Gene Structure in Eukaryotic Microbes. IRL Press, Oxford, pp 93–139

Hadji Sfaxi I, Ezzine A, Coquet L, Cosette P, Jouenne T, Marzouki MN (2012) Combined proteomic and molecular approaches for cloning and characterization of copper-zinc superoxide dismutase (Cu, Zn-SOD2) from garlic (*Allium sativum*). Mol Biotechnol 52:49–58

Harris N, Costa V, MacLean M, Mollapour M, Moradas-Ferreira P, Piper PW (2003) MnSOD overexpression extends the yeast chronological (G_0) life span but acts independently of Sir2p histone deacetylase to shorten the replicative life span of dividing cells. Free Radic Biol Med 34:1599–1606

Holley AK, Bakthavatchalu V, Velez-Roman JM, St Clair DK (2011) Manganese superoxide dismutase: guardian of the powerhouse. Int J Mol Sci 12:7114–7162

Holley AK, Dhar SK, Xu Y, St Clair DK (2012) Manganese superoxide dismutase: beyond life and death. Amino Acids 42:139–158

Hwang CS, Baek YU, Yim HS, Kang SO (2003) Protective roles of mitochondrial manganese-containing superoxide dismutase against various stresses in *Candida albicans*. Yeast 20:929–941

Iranzo O (2011) Manganese complexes displaying superoxide dismutase activity: a balance between different factors. Bioorg Chem 39:73–87

Jeong JH, Kwon ES, Roe JH (2001) Characterization of the manganese-containing superoxide dismutase and its gene regulation in stress response of *Schizosaccharomyces pombe*. Biochem Biophys Res Commun 283:908–914

Joh JH, Lee SH, Lee JS, Kim KH, Jeong SJ, Youn WH, Kim NK, Son ES, Cho YS, Yoo YB, Lee CS, Kim BG (2007) Isolation of genes expressed during the developmental stages of the oyster mushroom, *Pleurotus ostreatus*, using expressed sequence tags. FEMS Microbiol Lett 276:19–25

Kowluru RA, Kowluru V, Xiong Y, Ho YS (2006) Overexpression of mitochondrial superoxide dismutase in mice protects the retina from diabetes-induced oxidative stress. Free Radic Biol Med 41:1191–1196

Lee HJ, Kwon HW, Koh JU, Lee DK, Moon JY, Kong KH (2010) An efficient method for the expression and reconstitution of thermostable Mn/Fe superoxide dismutase from *Aeropyrum pernix* K1. J Microbiol Biotechnol 20:727–731

Lin CT, Tseng WC, Hsiao NW, Chang HH, Ken CF (2009) Characterization, molecular modelling and developmental expression of zebrafish manganese superoxide dismutase. Fish Shellfish Immunol 27:318–324

Liu J, Yin M, Zhu H, Lu J, Cui Z (2011) Purification and characterization of a hyperthermostable Mn-superoxide dismutase from *Thermus thermophilus* HB27. Extremophiles 15:221–226

Liu QL, Hang XM, Liu XL, Tan J, Li DT, Yang H (2012) Cloning and heterologous expression of the manganese superoxide dismutase gene from *Lactobacillus casei* Lc18. Ann Microbiol 62:129–137

Longo VD, Liou LL, Valentine JS, Gralla EB (1999) Mitochondrial superoxide decreases yeast survival in stationary phase. Arch Biochem Biophys 365:131–142

Ma A, Shan L, Wang N, Zheng L, Chen L, Xie B (2007) Characterization of a *Pleurotus ostreatus* fruiting body-specific hydrophobin gene, *Po.hyd*. J Basic Microbiol 47:317–324

Miriyala S, Holley AK, St Clair DK (2011) Mitochondrial superoxide dismutase - signals of distinction. Anticancer Agents Med Chem 11: 181–190

O'Brien KM, Dirmeier R, Engle M, Poyton RO (2004) Mitochondrial protein oxidation in yeast mutants lacking manganese- (MnSOD) or copper- and zinc-containing superoxide dismutase (CuZnSOD): evidence that MnSOD and CuZnSOD have both unique and overlapping functions in protecting mitochondrial proteins from oxidative damage. J Biol Chem 279:51817–51827

Park H, Ahn IY, Lee JK, Shin SC, Lee J, Choy EJ (2009) Molecular cloning, characterization, and the response of manganese superoxide dismutase from the Antarctic bivalve *Laternula elliptica* to PCB exposure. Fish Shellfish Immunol 27:522–528

Parker MW, Blake CC (1988) Iron- and manganese-containing superoxide dismutases can be distinguished by analysis of their primary structures. FEBS Lett 229:377–382

Ravindranath SD, Fridovich I (1975) Isolation and characterization of a manganese-containing superoxide dismutase from yeast. J Biol Chem 250:6107–6112

Sánchez C (2010) Cultivation of *Pleurotus ostreatus* and other edible mushrooms. Appl Microbiol Biotechnol 85:1321–1337

Schuren FHJ (1992) Regulation of gene expression during fruit-body development in *Schizophyllum commune*. University of Groningen, Dissertation

Song NN, Zheng Y, SJ E, Li DC (2009) Cloning, expression, and characterization of thermostable manganese superoxide dismutase from *Thermoascus aurantiacus* var. *levisporus*. J Microbiol 47:123–130

Wang M, Su X, Li Y, Jun Z, Li T (2010) Cloning and expression of the Mn-SOD gene from *Phascolosoma esculenta*. Fish Shellfish Immunol 29:759–764

Wu TH, Liao MH, Kuo WY, Huang CH, Hsieh HL, Jinn TL (2011) Characterization of copper/zinc and manganese superoxide dismutase in green bamboo (*Bambusa oldhamii*): Cloning, expression and regulation. Plant Physiol Biochem 49:195–200

Xie XQ, Wang J, Huang BF, Ying SH, Feng MG (2010) A new manganese superoxide dismutase identified from *Beauveria bassiana* enhances virulence and stress tolerance when over-expressed in the fungal pathogen. Appl Microbiol Biotechnol 86:1543–1553

Yin CM, Chen YY, Zhu HY, Lei JH, Ma AM (2012) Cloning and quantitative analysis of genes specifically expressed in mycelium and primordium of *Pleurotus ostreatus*. In: Zhang JX, Wang HX, Chen MJ (eds) Mushroom Science XVIII: proceedings of the 18th congress of the international society for mushroom science. China Agriculture Press, Beijing, pp 161–167

Yin C, Zheng L, Chen L, Tan Q, Shang X, Ma A (2014) Cloning, expression, and characterization of a milk-clotting aspartic protease gene (*Po-Asp*) from *Pleurotus ostreatus*. Appl Biochem Biotechnol 172:2119–2131

Zhang Q, Li F, Wang B, Zhang J, Liu Y, Zhou Q, Xiang J (2007) The mitochondrial manganese superoxide dismutase gene in Chinese shrimp *Fenneropenaeus chinensis*: cloning, distribution and expression. Dev Comp Immunol 31:429–440